A computational study on the amine-oxidation mechanism of monoamine oxidase: Insight into the polar nucleophilic mechanism†

Safiye Sağ Erdem,*[a] Özlem Karahan,[a] İbrahim Yıldız‡[a] and Kemal Yelekçi[b]

Received 9th August 2005, Accepted 3rd January 2006
First published as an Advance Article on the web 23rd January 2006
DOI: 10.1039/b511350d

The proposed polar nucleophilic mechanism of MAO was investigated using quantum chemical calculations employing the semi-empirical PM3 method. In order to mimic the reaction at the enzyme's active site, the reactions between the flavin and the *p*-substituted benzylamine substrate analogs were modeled. Activation energies and rate constants of all the reactions were calculated and compared with the published experimental data. The results showed that electron-withdrawing groups at the *para* position of benzylamine increase the reaction rate. A good correlation between the log of the calculated rate constants and the electronic parameter (σ) of the substituent was obtained. These results agree with the previous kinetic experiments on the effect of *p*-substituents on the reduction of MAO-A by benzylamine analogs. In addition, the calculated rate constants showed a correlation with the rate of reduction of the flavin in MAO-A. In order to verify the results obtained from the PM3 method single-point B3LYP/6-31G*//PM3 calculations were performed. These results demonstrated a strong reduction in the activation energy for the reaction of benzylamine derivatives having electron-withdrawing substituents, which is in agreement with the PM3 calculations and the previous experimental QSAR study. PM3 and B3LYP/6-31G* energy surfaces were obtained for the overall reaction of benzylamine with flavin. Results suggest that PM3 is a reasonable method for studying this kind of reaction. These theoretical findings support the proposed polar nucleophilic mechanism for MAO-A.

Introduction

MAO catalyzes the oxidation of various amine neurotransmitters, such as serotonin, dopamine and norepinephrine.[1] It exists as two isozymic forms, MAO-A and MAO-B.[2,3] These two forms display different substrate and inhibitor specificities. However, it is believed that they catalyze substrate oxidation by the same mechanism. Compounds that selectively inhibit MAO-A exhibit antidepressant activity, whereas the ones that selectively inhibit MAO-B are used in the treatment of Parkinson's disease.[4] Other findings showed that MAO-B inhibitors have neuroprotective[5] and antioxidant effects,[6] as well as a role in delaying apoptotic neuronal death.[7]

MAO is a flavoenzyme in which the flavin is covalently attached at the 8α-methyl group to an enzyme active-site cysteine residue.[8] It catalyzes the anaerobic oxidation of amine substrates to the corresponding imines, which are hydrolyzed to aldehydes nonenzymatically. The flavin is reduced to the hydroquinone and converted back into the oxidized form by reaction with molecular oxygen, and the enzyme turns to its native form.

Over the years, there have been extensive efforts to understand the MAO-catalyzed amine-oxidation mechanism. Four basic mechanisms have been proposed so far[9]: a hydride mechanism, a carbanion mechanism, an addition–elimination (nucleophilic) mechanism, and a radical mechanism. According to the hydride mechanism, a hydride ion from the α-C of the amine migrates to the N5 atom of the flavin. This is unlikely to occur, because hydride transfer is a high-energy process. The carbanion mechanism involves the abstraction of an α-proton by an active-site base residue, forming a carbanion. This mechanism does not appear to be a favorable process, because the α-H is not acidic enough; the pK_a is greater than 30. In the addition–elimination mechanism proposed previously, the amine nitrogen atom of the substrate attacks one of the electrophilic sites of the flavin: C2, C4a, or N5. This step is followed by deprotonation and β-elimination with an active-site base residue. Silverman[9] argues against this because such a mechanism may violate the principle of microscopic reversibility. Silverman's groups[10a] proposed radical mechanisms for MAO-B. According to Silverman, a one-electron transfer from the amino group to the flavin would give the amine radical cation, which can lose a proton to give the carbon radical. Since the pK_a of the α-proton of an amine radical is about 10, the enzyme can remove this proton readily. The radical generated by deprotonation can be oxidized further by a second electron transfer or by radical combination with an active-site radical followed by β-elimination to the immonium ion. The basis for this mechanism is derived from single-electron-transfer (SET) chemistry observed in the oxidation of amines and also from

[a]*Chemistry Department, Marmara University, Faculty of Arts and Sciences, 34722, Göztepe, Istanbul, Turkey. E-mail: erdem@marmara.edu.tr; Fax: +90 216 3478783; Tel: +90 216 3479641*
[b]*Kadir Has University, Faculty of Arts and Sciences, 34230, Cibali, Istanbul, Turkey*

† Electronic supplementary information (ESI) available: Total energies, zero point vibrational energies, enthalpies and Gibbs free energies (kcal mol^{-1}) of PM3 optimized structures for the polar nucleophilic mechanism of *p*-X-benzylamines (X = H, OCH_3, CF_3, NO_2, $N(CH_3)_2$, Cl, OH, Br, I, F). See DOI: 10.1039/b511350d

‡ Present address: Center for Supramolecular Science, Department of Chemistry, University of Miami, 1301 Memorial Drive, Florida, 33146-0431, USA.

ring-opening and SET chemistry observed in chemical model studies of MAO-B.[1] The argument against this mechanism was the failure to detect a radical intermediate species of catalytic significance in either MAO-A or MAO-B, but very recently, Rigby *et al.*[10b] presented spectroscopic evidence consistent with the presence of a stable tyrosyl radical in partially reduced human MAO-A. Other negative evidence is that a single electron transfer from the amine substrate to the flavin is thermodynamically unfavorable.[11] However, Silverman upholds the argument that the intrinsic binding, which could distort the bonds of amine and flavin, would lower the redox potentials of the amine and the flavin.[4,9,12] According to a number of arguments, large apparent barriers to electron transfer might not prevent the reaction in an enzyme active site.[9b]

Recently, elucidation of the structure of human MAO-B[13a] and rat MAO-A[13b] by X-ray has provided new insights into the MAO mechanism. According to the crystal structure, there is no active-site base residue that could facilitate proton abstraction from the α-C of the amine. On the basis of this result, Silverman[12] revised the radical mechanism, and Edmondson[14] revised the addition–elimination mechanism. In both of these modified mechanisms, the base that can abstract the α-proton of the amine is the N5 atom of the flavin instead of an active-site base residue. Thus, the flavin itself acts as the base (Fig. 1 and Fig. 2).

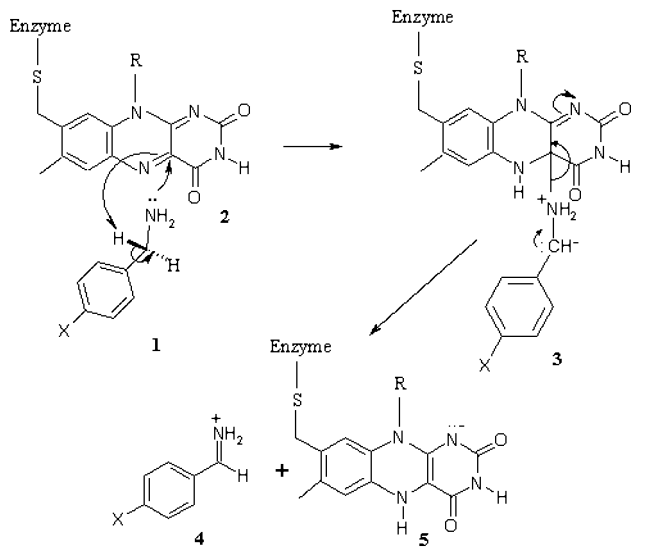

Fig. 1 Modified polar nucleophilic mechanism proposed by Miller and Edmondson.[14]

Miller and Edmondson[14] determined the reaction rates and binding affinities of 17 *p*-substituted benzylamine analogues with recombinant human liver MAO-A by steady-state and stopped-flow kinetic experiments. SAR analysis shows a strong correlation between the rate of flavin reduction and electronic effects (σ) of the substituent, such that electron-withdrawing substituents increase the rate of flavin reduction with a large positive ρ value. In addition, they found large deuterium kinetic isotope effects. In a similar study[15] on mitochondrial bovine liver MAO-B, quantitative-structure–activity-relationship derived from the reaction rates of a series of *p*-and *m*-substituted benzylamine analogues with MAO-B shows no apparent dependence of the limiting rate of flavin reduction on the electronic properties of the substituent. These results strongly support a proton-abstraction mechanism involving an α-C–H bond cleavage. The data are inconsistent with a direct H atom abstraction or hydride transfer mechanism, but are consistent with the aminium cation radical mechanism proposed by Silverman, as well as the polar nucleophilic mechanism put forward by Edmondson. In order to clarify these findings and the enzyme mechanism, we performed quantum chemical modeling of the uncatalyzed reactions of *p*-substituted benzylamines with the flavin ring, shown in Fig. 1. It is not possible to perform quantum chemical calculations on the enzyme because of the size of the system. Besides, information about the simple flavin-catalyzed reaction is also required to gain a deeper understanding of the enzyme catalysis. Therefore, we chose the reaction that occurs between the flavin, *e.g.*, the isoalloxazine ring and the *p*-substituted benzylamines to investigate the simple flavin-catalyzed reaction.

The enzyme reaction is expected to follow the general mechanism shown below.

$$\text{E-FAD}_{ox} + \text{S} \rightleftharpoons \text{E-FAD}_{ox}\text{–S} \rightarrow \text{E-FAD}_{red}\text{–imine} \rightarrow \text{E-FAD}_{red} + \text{imine}$$

Initially, the enzyme, E-FAD_{ox}, binds to the substrate, S, to form the enzyme–substrate complex, E-FAD_{ox}–S (reactant complex). Then the reaction takes place between FAD and the substrate. FAD is reduced while the amine substrate is converted to the imine. At first, a product complex, E-FAD_{red}–imine, is formed, and then the complex dissociates. In accordance with this mechanism, we performed geometry optimizations for the stationary points along the reaction coordinate of the polar mechanism shown in Fig. 1. The geometries and the energies of the substituted benzylamines, *p*-X (X = H, OCH_3, OH, $N(CH_3)_2$, F, Cl, Br, I,

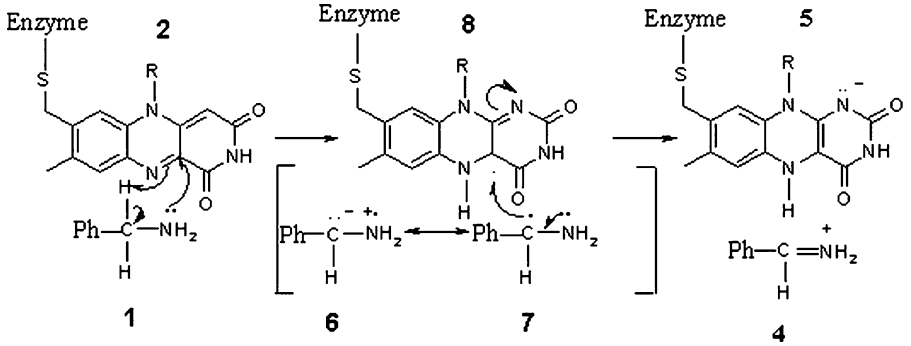

Fig. 2 Modified radical mechanism proposed by Silverman *et al.*[12]

CF_3, NO_2), the flavin, their reactant complexes, their transition-state structures, their product complexes, and the products were calculated.

Although a considerable amount of work has been accumulated in the literature, the mechanism of amine oxidation by MAO is still not completely understood. The majority of the published work[16–41] involves experimental techniques such as isotopic labeling and kinetic measurements,[16–18] efforts for isolating and detecting reactive intermediates,[19–25] studies on mechanism-based inactivators,[26–40] and mutation studies.[12] Besides, there are a few articles that involve structure–activity relationships (SAR)[41–43] and theoretical[44] work. On the other hand, theoretical methods based on quantum chemical calculations can also supply important information and are widely used in elucidating various reaction mechanisms, but no such report exists in the literature for the MAO mechanism, except a thermodynamic reaction profiling related to Alzheimer's disease.[44c] Therefore, the present work is aimed at the investigation of the recently proposed polar mechanism of MAO by taking advantage of quantum chemical calculations. Modeling the radical mechanism is our ongoing work and will be published separately. For the proposed polar mechanism, we have run calculations using the semiempirical PM3[45] method. Semiempirical methods are intended for studying large molecular systems of chemical or biological interest because of the low cost. One of our future goals is to be able to examine the enzymatic reaction directly using a hybrid quantum mechanics and molecular mechanics (QM/MM) approach. Due to the large size of the system, the use of high-level *ab initio* and or density functional theory as the QM part would be prohibitive. On the other hand, QM/MM calculations that use semiempirical molecular orbital methods as the QM part are computationally very attractive and have been applied to several enzymes[46] including a few flavin-containing enzymes.[47] Although semiempirical methods are fast, they are not as reliable as time-consuming *ab initio* and DFT methods. Therefore we have done some test calculations using DFT methodology to verify the results of the PM3 model. It is known that molecular density functional calculations give remarkably accurate results for molecular structures and electronic properties. Furthermore, since they take electron correlation effects into account, the DFT results are of a quality comparable to the conventional post Hartree–Fock treatments.

Although semiempirical methods cannot produce reliable results for the quantitative treatment of molecular properties and energies, the anticipated errors are expected to be in the same direction of the discussed physical effect.[48] Therefore, the computed trends in a chemical family or their modification through a perturbation are, in general, correctly reproduced by semiempirical methods. Thus, in this study, we investigate the trend in the reaction rate with respect to *p*-substitution by various groups, which is expected to produce qualitatively reliable results. The correlation of calculated rates with the experimental rates of the enzyme is a reasonable approach to test the mechanism. Ridder *et al.*[47a,b] applied a similar approach to other flavoenzymes, using a semiempirical method in a combined QM/MM study. Among semiempirical methods, PM3 method was used successfully in modeling various enzyme reactions in the literature,[46b–g] including also FAD containing enzymes.[47c,d] Therefore, we have chosen PM3 method to investigate the mechanism of MAO.

Methodology

The Gaussian 98 program package[49] was used for all calculations. For the reaction of benzylamine with isoalloxazine ring, geometries of the reactants, products, and transition states were fully optimized using the semiempirical PM3,[45] *ab initio* HF/6-31G* theories, and a hybrid DFT (B3LYP functionals[50] with the 6-31G* basis set) method. Transition-state structures were characterized with one imaginary frequency corresponding to the stretching motion of the bonds being broken or formed. IRC (intrinsic reaction coordinate)[51] calculations were also performed for all transition-state structures, and the structures corresponding to the reactant complex and the product complex were identified. These were further optimized to obtain the reactant complex and the product complex structures.

For *p*-X-substituted benzylamines (X = H, OCH_3, OH, $N(CH_3)_2$, F, Cl, Br, I, CF_3, NO_2), thermodynamic calculations were performed with the PM3 method at two different temperatures, 10.9 °C and at 25 °C which were used in experimental work. Rate constants were calculated according to the well-known equation[52]:

$$k = \frac{k_b T}{hc} e^{-\Delta G^*/RT}$$

where k = rate constant, k_b = Boltzmann constant, T = temperature, ΔG^* = free energy of activation, h = Planck constant, c = concentration (taken as unity), R = gas constant.

Single-point energy calculations at the B3LYP/6-31G* level using PM3 geometries were also employed for comparison.

Results and discussion

1. PM3 Calculations

Structures and energies. Since the optimized structures related to the reactions of *p*-substituted benzylamines are very similar to those of benzylamine, only the reactions of benzylamine will be discussed in this section.

The modified polar nucleophilic (or addition–elimination) mechanism[14] in Fig. 1 consists of two steps. The first step is the addition reaction in which the formation of a flavin 4a adduct, **3**, is proposed to occur by the attack of nonbonding electrons of the amine, **1**, to the 4a carbon of the flavin, **2**. This attack increases the basicity of the isoalloxazine ring at the N5 position of the flavin. A concerted transfer of the benzyl proton to the N5 of flavin is thus facilitated. The second step is the elimination to produce the imonium ion, **4**, and the reduced flavin, **5**, which is then reoxidized by molecular oxygen.

In order to model the bimolecular polar mechanism in Fig. 1, we optimized the structures of the reactants, reactant complexes, transition states, adducts, and products shown in Fig. 3(a) and (b). Important geometrical parameters of the optimized structures for the reaction of benzylamine with flavin are given in Table 1. Similar structural features were also observed for the reactions of *p*-substituted benzylamines; therefore, their values are not given. All the dihedral angles in isolated oxidized FAD are very close to 0° or 180° (only two of them are given), indicating that it has a planar structure. However, reduced FAD is bent by about 25° out of that plane; dihedral angles are around 155° and 25°. These results are in agreement with earlier reports.[53] In the reactant complex, an intermolecular H-bond between N11 and the proton

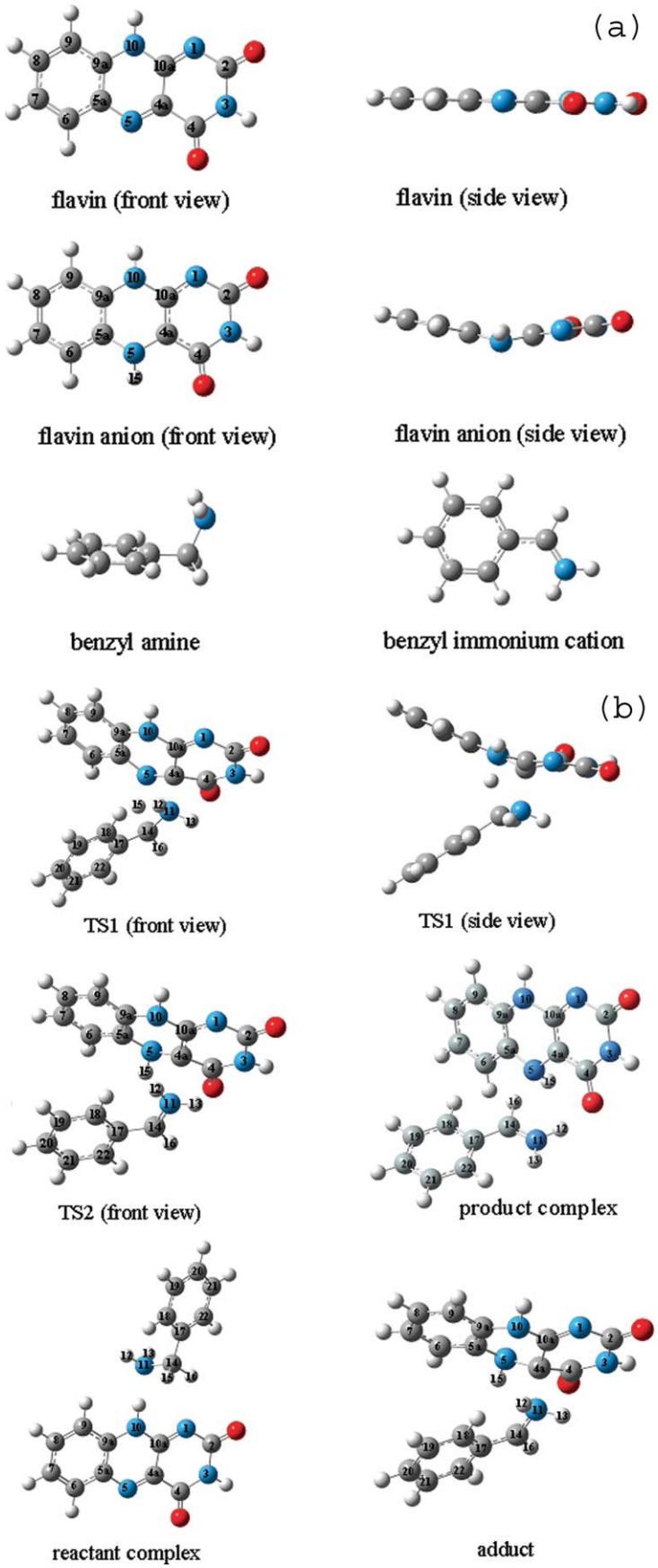

Fig. 3 (a) 3-D view of the PM3 optimized structures for the reactants and products. (b) 3-D view of the PM3 optimized structures; reactant complex, transition states, adduct, and product complex.

Table 1 Selected geometrical parameters of the optimized structures for the polar reaction of benzylamine with flavin, calculated at PM3 level

	Amine	FAD	Iminium ion	FAD^-	Reactant complex	TS1	Adduct	TS2	Product complex
Distances/Å									
N1–C10a		1.317		1.358	1.322	1.319	1.313	1.324	1.339
C10a–C4a		1.469		1.395	1.468	1.503	1.505	1.447	1.413
C4a–N5		1.307		1.450	1.309	1.427	1.474	1.455	1.459
N5–H15				0.995	5.973	1.328	1.001	0.997	1.000
H15–C14	1.070				1.110	1.477	2.561	2.906	3.251
C14–N11	1.476		1.320		1.494	1.439	1.369	1.322	1.304
N11–C4a					5.597	1.729	1.716	2.247	3.714
C14–C17	1.500		1.435		1.498	1.464	1.440	1.453	1.453
Bond angles/°									
C4a–N5–C5a		120.1		114.5	119.9	118.1	116.4	116.5	115.1
C4a–N5–H15					58.6	101.0	111.3	111.5	108.3
N5–C4a–N11					107.2	103.2	110.8	105.8	67.9
N5–H15–C14					90.0	128.2	101.3	107.2	58.1
H15–C14–N11	107.8				108.0	96.0	82.9	83.9	98.9
C14–N11–C4a					100.8	107.1	114.1	111.2	70.8
H16–C14–N11			118.8		107.7	114.6	119.1	119.0	116.0
Dihedral angles/°									
C6–C5a–N5–C4a		180.0		157.4	180.0	−177.2	−160.5	−167.4	174.9
C5a–N5–C4a–C4		180.0		−155.4	180.0	−145.0	−163.2	−170.6	−176.2
C5a–N5–H15–C14					−106.6	−109.9	−97.5	−94.7	−123.9
N5–H15–C14–N11					51.7	−3.3	−13.8	−11.2	−115.0
N5–H15–C14–C17	32.7				175.6	120.3	108.7	112.6	85.7
H15–C14–C17–C18					−36.8	−96.1	−94.4	−89.7	−20.5
N5–C4a–N11–C14					129.7	20.0	37.5	38.7	−35.4
C4a–N11–C14–H15					−75.6	−10.0	−13.5	−13.5	32.9
H16–C14–C17–C18			0.0		−154.7	153.3	171.3	173.8	4.8

of N10 is observed, which holds the two molecules together. In the first transition state (TS1), a five-membered ring structure involving C4a, N5, H15, C14, N11 forms. This ring is almost orthogonal to the planes of the flavin and the substrate as shown in TS1 (side view). The phenyl groups in TS1, adduct, and TS2 are directed towards the benzene moiety of the flavin to increase π–π interaction.

The H15–C14 bond length in the reactant complex is 1.11 Å. It stretches to 1.48 Å in TS1 and is broken in the adduct, while the N5–H15 distance shortens to 1.33 Å and 1.00 Å in TS1 and in the adduct, respectively, confirming the removal of α-H by the N5 atom of flavin. In parallel to this, the N11–C4a distance decreases to 1.73 Å in TS1 and to 1.71 Å in the adduct; the C4a–N5 distance increases from 1.31 Å to 1.43 Å and 1.47 Å along the reaction coordinate from the reactant to TS1 and the adduct. These changes are consistent with the bond-breaking and bond-forming processes in the first step shown in Fig. 1. In the second step, as a new π-bond forms between C14 and N11, the single bond between N11 and C4a is broken. This is observed from the shortening of the C14–N11 and the elongation of N11–C4a distances in TS2 relative to the ones in the adduct. The unusually long bond distance of N11–C4a in the adduct can be due to the steric constrains exerted by the isoalloxazine ring. The predicted bond angles, and especially the large value of C14–N11–C4a, also indicate the importance of steric repulsions in the adduct. Furthermore, flavin ring is bent by about 20° from planarity to overcome these repulsions.

Mulliken atomic charges of the selected atoms for each stationary point are given in Table 2. One can easily observe that the negative charge on C14 increases gradually along the first step of the reaction path and then decreases again at the second step since these electrons form a π-bond between C14 and N11 with the concomitant dissociation of the adduct. This feature of the reaction pathway, together with the observed changes in the geometrical parameters, show the formation of the adduct, indicating that the present model is in agreement with an addition–elimination type of mechanism as proposed by Miller and Edmondson.[14] In TS1 and adduct, the developing negative charge on C14 is delocalized over the substrate benzene ring, mainly at the *ortho* and *para* positions. In TS1, the atomic charge on H15 being transferred is +0.33, indicating that it really migrates as a proton. The total electronic charge on the flavin ring increases gradually along the reaction coordinate as expected. In the first step of the reaction, (from the reactant complex to the adduct), 0.21e of charge is transferred, whereas in the adduct dissociation step charge transfer is larger (0.51e). Overall, a net charge transfer of 0.73e is accomplished in going from the reactant complex to the product complex.

Energies of the optimized structures for the reaction of benzylamine and flavin are given in Table 3. Potential energy *versus* reaction coordinate diagram is shown in Fig. 4.

At the early stages of the reaction, a reactant complex (ES) is formed between the flavin and the benzylamine. The proposed polar mechanism involves two steps. The first step, in which the α-C–H bond is cleaved to produce an unstable covalent adduct, has a higher activation energy, including ZPE, than the second step by 40.976 kcal mol^{-1} (Table 3). Therefore, α-proton abstraction is the rate-determining step, which is in accordance with the results of Edmondson *et al.*[14] They reported that the deuterium kinetic isotope effects on k_{cat}, k_{red}, K_{cat}/K_m, and K_{red}/K_s varied between 6 and 13 in α,α-[^{2}H]benzylamines for both MAO-A and MAO-B, depending on the substrate. Formation of the adduct is a highly endothermic step (34.937 kcal mol^{-1}), and therefore the structure of TS1 and TS2 resemble that of the adduct, which is consistent with the Hammond postulate. The adduct is quite unstable, only 2.687 and 10.402 kcal mol^{-1} lower in energy than

Table 2 Mulliken charges for selected atoms calculated from PM3 optimization

Atoms	Reactant complex	TS1	Adduct	TS2	Product complex
N1	−0.288	−0.270	−0.241	−0.303	−0.331
C2	0.339	0.326	0.323	0.328	0.334
N3	−0.168	−0.196	−0.171	−0.179	−0.120
C4	0.343	0.267	0.278	0.333	0.370
C4a	−0.184	−0.124	−0.347	−0.613	−0.608
N5	0.110	−.218	0.041	0.133	0.170
C5a	−0.150	0.002	−0.089	−0.096	−0.164
C6	−0.090	−0.185	−0.185	−0.220	−0.201
C7	−0.235	−0.169	−0.165	−0.175	−0.215
C8	−0.120	−0.201	−0.190	−0.207	−0.166
C9	−0.240	−0.173	−0.177	−0.189	−0.223
C9a	−0.067	−0.201	−0.155	−0.139	−0.062
N10	0.095	0.165	0.118	−0.071	0.090
C10a	0.023	−0.036	−0.011	0.084	0.138
N11	−0.094	0.577	0.880	0.572	0.281
H12	0.064	0.048	0.014	0.096	0.078
H13	0.082	0.056	0.027	0.109	0.237
C14	−.0223	−0.746	−0.904	−0.368	−0.237
H15	0.175	0.331	0.163	0.109	0.084
H16	0.134	0.235	0.283	0.263	0.354
C17	−0.147	0.024	0.099	−0.100	−0.169
C18	−0.168	−0.252	−0.279	−0.173	−0.109
C19	−0.190	−0.153	−0.145	−0.176	−0.203
C20	−0.182	−0.219	−0.241	−0.161	−0.135
C21	−0.192	−0.163	−0.158	−0.189	−0.196
C22	−0.181	−0.208	−0.227	−0.143	−0.147
Total flavin ring	−0.067	−0.482 (−0.151)[a]	−0.281	−0.741	−0.793

[a] Charge of H15 was included.

Table 3 Total energies (E_{el}), activation energies (ΔE^*), reaction energies (ΔE), and binding energy (ΔE_b) (kcal mol^{-1}) including zero point vibrational energy (ZPE) corrections, calculated from PM3 optimizations

	E_{el}	E_{el} + ZPE
Flavin,FAD, (E)	−13.850	80.282
Benzylamine (S)	19.821	109.991
Flavin anion, FAD$^-$	−90.640	11.003
Benzyl immonium (P)	194.546	271.771
Reactant complex (RC)	0.859	188.597
First transition state (TS1)	47.974	233.936
Adduct	33.551	223.534
Second transition state (TS2)	38.230	226.221
Product complex (PC)	17.920	206.032
$\Delta E_1{}^*$ ($E_{TS1} - E_{E+S}$)	42.003	43.663
$\Delta E_2{}^*$ ($E_{TS2} - E_{adduct}$)	4.679	2.687
ΔE_1 ($E_{adduct} - E_{reactant\ complex}$)	32.692	34.937
ΔE_2 ($E_{product\ complex} - E_{adduct}$)	−15.631	−17.502
ΔE ($E_{product\ complex} - E_{E+S}$)	11.949	15.759
ΔE_b ($E_{E+S} - E_{reactant\ complex}$)	5.112	1.676

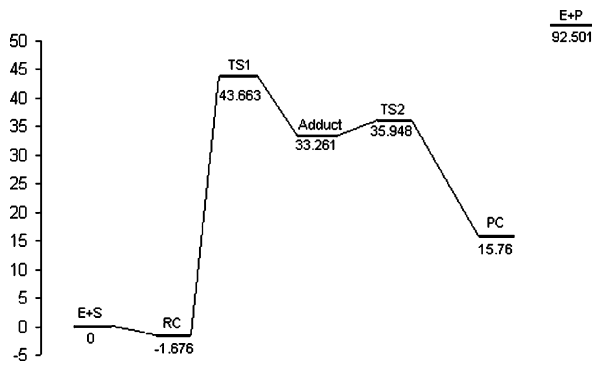

Fig. 4 Calculated potential energy surface with the PM3 method. Energies include ZPE corrections and are relative to E + S. E + S represents flavin (FAD) + benzylamine; RC represents the reactant complex; PC represents product complex; E + P represents flavin anion (FAD $^-$) + benzyl immonium cation.

TS2 and TS1, respectively. As the adduct forms it can easily pass the low-energy barrier of 2.687 kcal mol^{-1} and dissociate into the products. Therefore, the experimental detection of the adduct is a challenging task. Using a rapid-scanning stopped flow apparatus, Miller and Edmondson[14] collected time-resolved absorption spectra during the anaerobic reduction of MAO-A and MAO-B. They found no evidence for the formation of any spectrally detectable intermediate, including the formation of either anionic or neutral flavin semiquinone or a flavin 4a adduct. They concluded that, if a chromogenic intermediate is formed during the reduction of MAO, its concentration must be less than 5% of the sum of the concentrations of the oxidized and reduced flavin to escape detection. However, flavin C4a nucleophile adducts were identified in both model systems and in other flavoenzyme systems.[54a] Recent structural data show that the C4a adduct also forms upon inhibition of MAO-B with *trans*-2-phenylcyclopropylamine.[54b,c]

The energies of the separated products (**4** and **5** in Fig. 1) have been predicted to be very high. This is because the charged species are destabilized in the gaseous phase for which the calculations have been performed. We tested this situation by repeating the calculations including the aqueous solvation effect. As we expected, the energies of the products decreased to reasonable values. In order to obtain more realistic results, the energy of the product complex was used instead of those of the separate products in calculating the reaction energies in Table 3. The

second step is exothermic by 17.502 kcal mol^{-1}, and the overall reaction is endothermic by 15.759 kcal mol^{-1}.

It is known that semiempirical calculations are not suitable for absolute activation energy calculations. Calculated values are usually (but not always) larger than experimental activation energies.[55] For example, in proton-transfer reactions, PM3 barriers of activation are about 5–10 kcal mol^{-1} higher than *ab initio* results.[56] Since the semiempirical theories are not good enough to produce the activation energies, the energies obtained here can only be considered qualitatively, but not with their absolute values.

Rate constants and substituent effects. Edmondson and co-workers applied steady-state and stopped-flow kinetic experiments and determined the limiting rate of enzyme reduction, k_{red}, for *p*-substituted benzylamine analogues using recombinant human liver MAO-A[14] at 10.9 °C and mitochondrial bovine liver MAO-B[15] at 25 °C. The concentration of the amine substrate was held at least 10-fold higher than that of the enzyme to ensure pseudo-first-order kinetic behavior during these experiments. To compare the results of our computational study with these experiments we calculated the first-order rate constants. Because the experiments were performed at two different temperatures, thermal corrections to Gibbs free energies were included in thermodynamic calculations. The rate constants obtained at 10.9 °C were compared with the results of MAO-A and the ones at 25 °C were compared with those of MAO-B. For the oxidation of various *p*-substituted benzylamines, free energies of activation used in the calculation of the rate constants are given in Table 4. Calculated and the experimental rate constants, together with the Hammett substituent parameters, σ, are listed in Table 5.

The effect of the substituent electronic parameters on the rate of flavin reduction has been examined. As it can be observed from Table 4 and Table 5, electron-withdrawing substituents *p*-NO_2 and *p*-CF_3, decrease the free energy of activation by about 1–1.6 kcal mol^{-1} relative to benzylamine and thus enhance the rate of α-C–H bond cleavage. The effect of the substituents has been further investigated by comparing the Mulliken charges and the bond distances of the critical atoms in the transition-state structures. As we discussed above, a negative charge develops at C14 in the transition state. In the optimized transition-state structures for *p*-NO_2- and *p*-CF_3-benzylamines, the electron density at C14 is higher (−0.752) than that for *p*-$N(CH_3)_2$-, *p*-OH-, and *p*-OCH_3-substituted ones (−0.734, −0.736, and −0.736, respectively). Meanwhile, the positive charge on H15 increases in *p*-NO_2- and *p*-CF_3-benzylamines (0.337 and 0.335, respectively) relative to the charge in *p*-$N(CH_3)_2$-, *p*-OH-, and *p*-OCH_3-substituted ones (0.328, 0.329, and 0.329, respectively). In parallel to this, the negative charge on flavin N5 increases in *p*-NO_2- (−0.227) and *p*-CF_3- (−0.224) substituted substrates relative to those that are *p*-$N(CH_3)_2$- (−0.212), *p*-OH- (−0.214), and *p*-OCH_3- (−0.214) substituted. Thus, in *p*-NO_2- and *p*-CF_3-benzylamines, the α-H exhibits more acidic character and the flavin N5 is more basic, which facilitates the deprotonation step relative to the electron-donating groups at the *p*-position. In addition, the increase in reaction rate is governed with the stabilization of the transition state for *p*-NO_2- and *p*-CF_3-benzylamines because the developing negative charge at C14 is delocalized over the benzene ring as a result of the electron-withdrawing effect of the *p*-substituents. This situation has been observed from the shortening of the C14–C17 bond distance as the substituent electron-withdrawing character increases. For example, in the transition-state structures of *p*-$N(CH_3)_2$-, *p*-OH-, *p*-OCH_3-, *p*-H-, *p*-CF_3- and *p*-NO_2-benzylamines the C14–C17 distances are 1.465, 1.466, 1.466, 1.464, 1.460, and 1.457 Å, respectively. In relation with this, N11–C4a distances also decrease with electron-withdrawing power of the substituent (1.740, 1.733, 1.736, 1.716, 1.659, and 1.636, respectively)

Table 4 Free energies of activation, ΔG^*/kcal mol^{-1} for the reactions of *p*-substituted benzylamine derivatives with flavin, calculated from PM3 method[a]

p-Substituent	$t = 10.9$ °C	$t = 25$ °C
$N(CH_3)_2$	50.106	49.527
OH	49.804	50.155
OCH_3	49.942	50.307
H	49.742	50.013
F	49.317	49.665
Cl	49.285	49.643
Br	49.439	49.808
I	49.279	49.639
CF_3	48.821	49.121
NO_2	48.106	48.553

[a] ΔG^* was calculated as the free energy of TS1—the free energy of the reactant complex.

Table 5 Experimental and calculated rate constants (s^{-1}), and electronic parameters of the substituents, σ, for the reactions of the *p*-substituted benzylamines with flavin, calculated from PM3 method

		Experimental k_{red}		Calculated k_{red}	
p-Substituent	σ	MAO-A Ref. 14	MAO-B Ref. 15	k^a $t = 10.9$ °C	k^b $t = 25$ °C
$N(CH_3)_2$	−0.63	0.041	2.467	1.65	30.62
OH	−0.38	0.057	1.950	2.81	10.61
OCH_3	−0.12	0.013	6.083	2.20	8.21
H	0.00	0.024	12.667	3.14	13.48
F	0.15	0.049	10.000	6.67	24.26
Cl	0.24	0.132	5.133	7.06	25.17
Br	0.26	0.195	2.050	5.37	19.06
I	0.28	0.313	—	7.14	25.34
CF_3	0.53	0.668	0.1920	15.95	60.76
NO_2	0.81	0.207	0.063	57.03	158.54

[a] Calculated $k \times 10^{-26}$. [b] Calculated $k \times 10^{-25}$.

Table 6 Statistical output of the correlation analysis shown in Fig. 5 and Fig. 6

Case	Equation	r^a	F^b	P^c	N^d
Fig. 5	$y = 1.00x + 0.66$	0.93	49.22	1.11×10^{-4}	10
Fig. 6	$y = 0.04x - 0.09$	0.93	43.84	2.98×10^{-4}	9

[a] Represents the correlation coefficient. [b] The F value is a statistical term relating the residuals of each point to the fitted line to the residuals of each line to the mean value. The higher the F value, the better the fit. [c] The significance is calculated from the P value and represents the fractional chance that the derived correlation is meaningless. [d] Represents the number of data points used in the regression.

Linear regression analysis of log k as a function of substituent parameter gave a good correlation ($r = 0.93$) with σ as shown in Fig. 5. The statistical output of this analysis was tabulated in Table 6. These results are in very good agreement with the linear regression analysis of Miller and Edmondson[14] for the substituent effect on MAO-A reduction rates. They reported a correlation coefficient of 0.89 after excluding some anomalously behaving substituents, such as OH, $N(CH_3)_2$, NO_2, and acetyl. These substituents are unique in that they can serve as π-electron donors or acceptors. Furthermore, these four anomalously behaving benzylamine analogues also exhibit a correlation of flavin reduction rates with σ, yielding a correlation coefficient of 0.99. Since very similar results have been obtained for the substituent effect with the MAO-A reduction rates and with the theoretically modeled polar mechanism, the mechanism of amine oxidation by MAO-A seems to be in accordance with the polar nucleophilic mechanism.

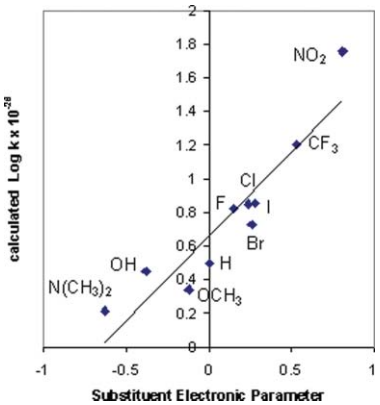

Fig. 5 Plot of calculated log k *versus* Hammett substituent parameter, σ.

We performed another linear regression analysis of the limiting rate of flavin reduction in MAO-A, k_{red}, with the calculated rate constants of the theoretically modeled polar mechanism at 10.9 °C (Fig. 6). A good correlation with $r = 0.93$ was obtained when the data point belonging to p-NO_2-benzylamine was excluded since this point was observed as an outlier with the standardized residual value of 2.66 in our statistical analysis. (Number of outliers lower than 10% of the general data are classically accepted in the literature as a threshold limit value for outliers' extraction.) The reason for NO_2 to be an outlier is that its experimental reduction rate is much smaller (Table 5) than the expected value when strong electron-withdrawing nature of this substituent is considered. Therefore, this data point was excluded in the experimental QSAR

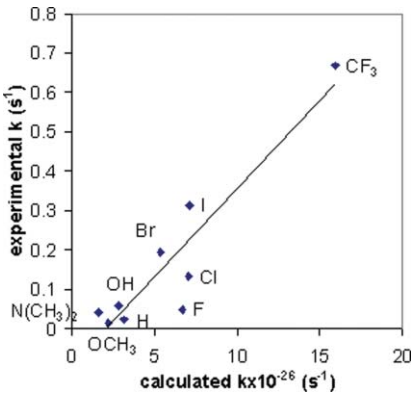

Fig. 6 Plot of calculated k *versus* the experimental rate of flavin reduction.

analysis[14] as discussed in the previous paragraph. The statistical significance of our correlation analysis is also given in Table 6. The correlation between the experimentally derived rate constants with those of the calculated ones is good enough to reveal that MAO-A most probably operates with a polar nucleophilic mechanism.

We have attempted a similar regression analysis of the limiting rate of flavin reduction in MAO-B, k_{red}, at 25 °C, with the calculated rate constants of the theoretically modeled polar mechanism. Since the two isozymic forms, MAO-A and MAO-B, are thought to oxidize their substrates with the same mechanism, we expected to get a similar correlation. To our surprise, we obtained a very low correlation. This finding can be interpreted in two different ways: (1) The mechanism of amine oxidation by MAO-A and MAO-B may not be the same, and the function of MAO-B may follow a different mechanism than the polar one, *e.g.*; the radical mechanism. This proposal requires evidence, but Silverman, the defender of the radical mechanism, used MAO-B and not MAO-A in many of his published works. (2) If the two isozymic enzymes operate with the same mechanism as expected, the lack of correlation between MAO-B reduction rates and the calculated values for the polar mechanism may be the result of insufficient modeling of the steric constraints of the bound substrate in the active site of MAO-B. Such steric constraints are known to be dominating in MAO-B.[41,57] One of our future goals is to investigate this situation using a QM/MM type of modeling of MAO-B catalysis.

2. DFT and *ab initio* calculations

In order to test PM3 results, the following calculations were done sequentially: *i.* We calculated the activation energies for the reactions of *p*-substituted benzylamines using single-point B3LYP/6-31G* calculations on the PM3 optimized geometries, in order to investigate the substituent effect. *ii.* Stationary points on the PM3 energy surface were re-calculated by single-point energies at the B3LYP/6-31G* and B3LYP/6-31 + G** levels. *iii.* Geometry optimizations and IRC calculations were carried out at the B3LYP/6-31G* level to map out the potential energy surface for the reaction of benzylamine with flavin. *iv.* The structure of the adduct and TS2 were optimized at the HF/6-31G* level, and the activation barrier was predicted.

Activation energies calculated by single-point energies at the B3LYP/6-31G* level are given in Table 7. Although these activation energies do not show a direct relationship with the

Table 7 Total electronic energies and activation energies[a,b], au, obtained from single point B3LYP/6-31G*//PM3 calculations

	Reactant complex		TS			
p-Substituent	E_{el}	ZPE[b]	E_{el}	ZPE[b]	ΔE^*	$\Delta E^* + ZPE$
$N(CH_3)_2$	−1215.034338	0.371913	−1214.930536	0.368377	0.103803	0.100267 (62.918)
OH	−1156.289979	0.303795	−1156.185643	0.301594	0.104335	0.10214 (64.089)
OCH_3	−1195.595728	0.330230	−1195.492024	0.328186	0.103704	0.101660 (63.792)
H	−1081.080193	0.299184	−1080.971379	0.296352	0.108814	0.10592 (66.503)
F	−1180.308226	0.291568	−1180.203172	0.289598	0.105055	0.103085 (64.686)
Cl	−1540.668902	0.289112	−1540.564573	0.287167	0.104328	0.102383 (64.246)
Br	−3652.177670	0.288719	−3652.073195	0.286779	0.104475	0.102535 (64.341)
CF_3	−1418.102020	0.305713	−1418.006643	0.303535	0.095377	0.093199 (58.482)
NO_2	−1285.560269	0.301861	−1285.471322	0.300548	0.088946	0.088933 (55.806)

[a] Unit in parenthesis is kcal mol^{-1}. [b] ZPE values obtained from PM3 harmonic vibrations were used.

electronic nature of the *p*-substituent (because geometries were not optimized), there is an apparent reduction in the activation energies of *p*-NO_2 and *p*-CF_3 susbtituted benzylamines. This result is in agreement with the predictions of PM3.

The potential energy surface obtained from single-point energy calculations at the B3LYP/6-31G* and B3LYP/6-31+G** levels on PM3 geometries is given in Fig. 7. Both calculations produced very similar results. The striking feature of these surfaces is that the adduct is extremely unstable and there is no barrier for the dissociation of the adduct. To investigate this feature in detail, we fully optimized the geometry of TS1 at the B3LYP/6-31G* level. Reactant and product complexes were obtained upon optimizing the identified structures from IRC calculations. The calculated B3LYP/6-31G* potential energy surface and the optimized geometries are shown in Fig. 8 and 9, respectively.

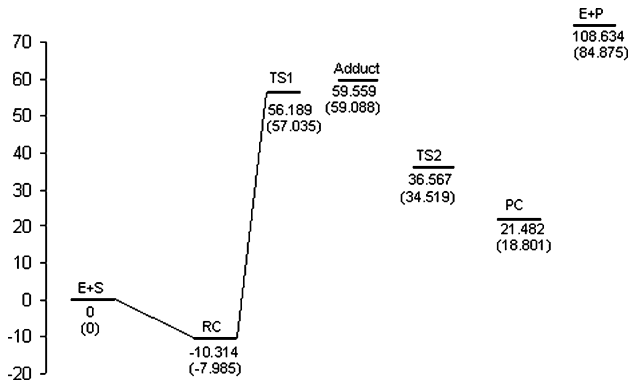

Fig. 7 Calculated potential energy surface with the single-point B3LYP/6-31G*//PM3 and B3LYP/6-31+G**//PM3 (in parentheses) methods. Energies include ZPE corrections calculated from PM3. E + S represents flavin (FAD) + benzylamine; RC represents the reactant complex; PC represents product complex; E + P represents flavin anion (FAD^-) + benzyl immonium cation.

Overall, the potential energy surface resembles the PM3 surface with the exception that no minimum corresponding to the adduct was located at B3LYP/6-31G* level. All our attempts to optimize an adduct structure have failed. It seems that this is related with the nature of the transition state because the N11–C4a distance is much longer (by 1.1 Å) than the distance in the PM3 transition state and the forming N5–H15 bond is 0.3 Å shorter

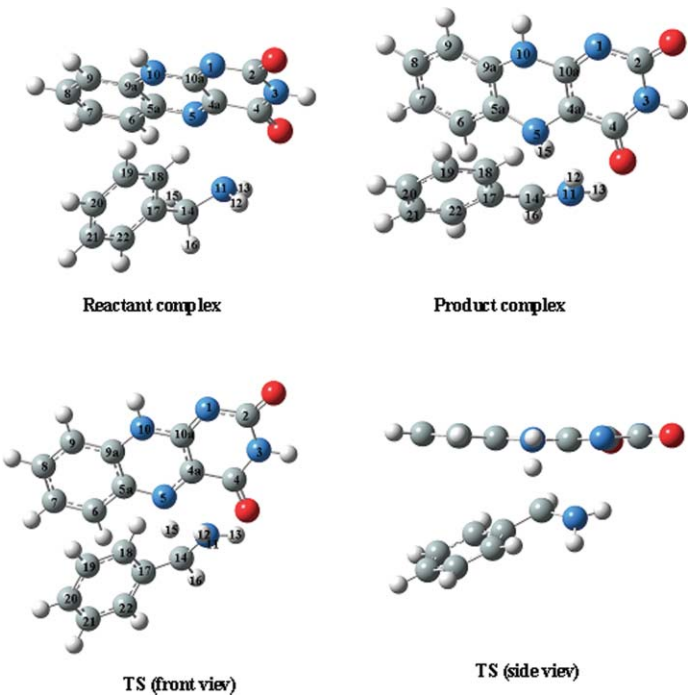

Fig. 8 3-D view of the B3LYP/6-31G* optimized structures; reactant complex, transition state, and product complex.

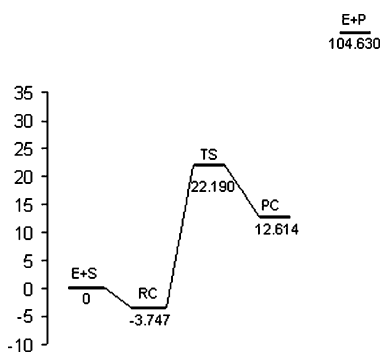

Fig. 9 Calculated potential energy surface at the B3LYP/6-31G* level. Energies include ZPE corrections and are relative to E + S. E + S represents flavin (FAD) + benzylamine; RC represents the reactant complex; PC represents product complex; E + P represents flavin anion (FAD^-) + benzyl immonium cation.

Table 8 Selected geometrical parameters of the optimized structures for the polar reaction of benzylamine with flavin, calculated at B3LYP/6-31G* level

	Amine	FAD	Iminium ion	FAD^-	Reactant complex	TS	Product complex
Distances/Å							
N1–C10a		1.372		1.335	1.370	1.312	1.319
C10a–C4a		1.466		1.382	1.465	1.435	1.406
C4a–N5		1.298		1.429	1.297	1.361	1.414
N5–H15				1.014	3.035	1.182	1.018
H15–C14	1.096				1.099	1.491	2.647
C14–N11	1.474		1.309		1.465	1.384	1.329
N11–C4a					3.131	2.804	2.894
C14–C17	1.519		1.425		1.519	1.460	1.446
Bond angles/°							
C4a–N5–C5a		119.0		118.3	118.9	117.5	117.5
C4a–N5–H15					94.4	109.3	110.7
N5–C4a–N11					96.4	82.9	75.2
N5–H15–C14					126.1	154.2	65.9
H15–C14–N11	107.3				106.8	100.6	99.2
C14–N11–C4a					106.3	88.6	84.5
H16–C14–N11	107.3		114.8		113.6	114.9	114.9
Dihedral angles/°							
C6–C5a–N5–C4a		180.0		159.4	179.8	176.9	162.9
C5a–N5–C4a–C4		180.0		−155.0	179.3	−175.8	−161.4
C5a–N5–H15–C14					−131.8	−93.4	−119.4
N5–H15–C14–N11					−17.7	−27.0	−83.6
N5–H15–C14–C17					104.5	98.6	54.0
H15–C14–C17–C18	32.7				−97.8	−87.6	−106.6
N5–C4a–N11–C14					−37.3	7.7	−10.2
C4a–N11–C14–H15					25.0	1.1	28.4
H16–C14–C17–C18			0.0		−33.6	172.3	−178.8

than the breaking H15–C14 bond (Table 8). The remaining characteristics of the transition state resemble closely the first transition state of the PM3 surface. Imaginary frequencies are 1782i and 1054i cm^{-1} for PM3 and B3LYP/6-31G*, respectively. The atoms, which contribute to the imaginary harmonic frequency, are the same in each transition structure. The geometrical change at C14 and N11 from a tetrahedral to a nearly planar structure accompanies the bond-formation and bond-cleavage, indicating the delocalization of the negative charge. This is observed in both transition structures, but is more pronounced in the TS of B3LYP/6-31G*. Thus, the transition state on the B3LYP/6-31G* surface corresponds to the first transition state on the PM3 surface, but it is a later TS, since H15 is closer to N5 in comparison to the case in the TS1 of the PM3 surface. Analogously, charge transfer from benzylamine to flavin is 0.26e more than the transfer in the first step of PM3 (Tables 2 and 9). However, it is 0.25e less than the overall charge transfer in PM3 because N11 is not as close to C4a as in the TS1 of the PM3 surface. It is expected that a shorter N11–C4a distance will enhance the charge transfer from amine N11 to C4a of the flavin and favor the formation of an adduct as well. A strong electron-withdrawing group should decrease N11–C4a distance as observed from PM3 calculations. For example, when a formyl group was replaced by the phenyl ring of benzylamine, N11–C4a distance in TS predicted by B3LYP/6-31G* calculations has decreased to 2.61 Å because of the relatively small size of the formyl group and its electron-withdrawing character.

Zheng and Bruice[46g] investigated the dehalogenation mechanism of 4-chlorobenzoyl CoA by 4-chlorobenzoyl CoA dehalogenase by modeling the nonenzymatic nucleophilic aromatic substitution (S_NAr) reaction between 4-Cl-Ph-CO-SCH_3 and CH_3COO^-. Similar to our case, they could not locate a Meisenheimer intermediate (σ-complex) on the HF/6-31G* and B3LYP/6-311+G** surfaces. However, a very shallow minimum corresponding to a Meisenheimer intermediate was located on the PM3 surface. They suggested that the Meisenheimer intermediate

Table 9 Mulliken charges for selected atoms calculated from B3LYP/6-31G* optimization

Atoms	Reactant Complex	TS	Product Complex
N1	−0.589	−0.597	−0.603
C2	0.706	0.691	0.682
N3	−0.683	−0.685	−0.683
C4	0.642	0.596	0.550
C4a	0.230	0.212	0.178
N5	−0.533	−0.678	−0.768
C5a	0.249	0.281	0.324
C6	−0.156	−0.168	−0.198
C7	−0.136	−0.135	−0.139
C8	−0.128	−0.131	−0.134
C9	−0.180	−0.191	−0.197
C9a	0.404	0.395	0.366
N10	−0.758	−0.781	−0.772
C10a	0.584	0.556	0.514
N11	−0.751	−0.683	−0.683
H12	0.307	0.344	0.364
H13	0.329	0.369	0.400
C14	−0.203	−0.221	0.053
H15	0.162	0.315	0.348
H16	0.132	0.197	0.178
C17	0.139	0.203	0.186
C18	−0.189	−0.188	−0.183
C19	−0.137	−0.128	−0.125
C20	−0.131	−0.130	−0.122
C21	−0.130	−0.122	−0.127
C22	−0.181	−0.193	−0.175
Total flavin ring	−0.010	−0.443 (−0.128)[a]	−0.483

[a] Charge of H15 was included.

could become much more stable in the active site where the negative charge in the Meisenheimer intermediate could be effectively stabilized by the amide hydrogens of Phe64 and Gly114. Indeed, Xu *et al.*,[46a] found a metastable Meisenheimer intermediate stabilized by hydrogen bonds with the expected amide hydrogens, in a QM/MM study calculated at the PM3/CHARMM level. In addition, Dong *et al.*[58] were able to obtain a stable Meisenheimer intermediate in HF and DFT optimizations with electron-withdrawing fluoro/nitro-substituents. These results indicated that the PM3 method was more accurate relative to DFT results for such S_NAr reactions. The nucleophilic addition reaction that we study is quite similar to the S_NAr reaction discussed above in the way that a negative charge develops at the transition state and in the adduct. Thus, it seems that PM3 results mimic the overall reaction path better than DFT calculations.

In order to check the existence of an adduct at a different level of theory, especially when diffuse functions are included in the basis set, we employed HF/6-31G* and HF/6-31++G* optimizations. Indeed, both levels found adduct structures which are very similar in geometry, having the critical N11–C4a and C14–N11 bond lengths as 1.52 Å and 1.53 Å, respectively, with some distortions in the flavin ring. However, this adduct is quite unstable and it dissociates very easily to give the reduced flavin and immonium cation. We were also able to locate a transition structure for the elimination step at the HF/6-31G* level. The dissociation barrier is extremely low; 1.92 and 3.14 kcal mol^{-1} with and without ZPE correction, respectively. The PM3 prediction (2.69 kcal mol^{-1}) for the same barrier is in perfect agreement with the HF/6-31G* level.

Since the first step is the rate-determining step with a high activation energy, the reaction rate depends on the stability of the adduct. Although such an intermediate is very unstable according to the gas phase calculations, it is likely that it may become much more stable in the active site where the charge in the adduct can be effectively stabilized by the favorable interactions supplied by the amino acid residues or backbones. Besides, the structure of the flavin ring in MAO is bent approximately 30° from planarity,[54c] whereas the aromatic isoalloxazine ring of free flavin is planar. Bent flavin in MAO is expected to facilitate the formation of the C4a adduct since such a flavin structure would diminish the repulsions of the approaching substrate.

Energies related to the optimized structures on the B3LYP/6-31G* surface (Fig. 9) are given in Table 10. Except for the absence of an intermediate, the remaining features resemble closely the PM3 surface (Fig. 4). Both PM3 and B3LYP/6-31G* calculations predict an endothermic reaction with ΔE values of 12.6 and 15.8 kcal mol^{-1}, respectively. The energy barrier predicted by B3LYP/6-31G* calculations is about 20 kcal mol^{-1} lower than the initial barrier calculated by the PM3 method. PM3 probably overestimated this barrier, since semiempirical methods give artificially large activation energies, especially for proton transfers.[46c,47b,56] The gas-phase activation barrier (22 kcal mol^{-1}) calculated at B3LYP/6-31G* level reveals that such a reaction can occur under normal conditions. However, it is likely that the same reaction can take place much faster in the enzyme active site. The MAO substrate cavity has the shape of an elongated disc perpendicular to the flavin ring. The amino acid residues lining the substrate cavity are mostly aromatic and aliphatic, which provides a hydrophobic environment. The more polar area where the amine would preferentially bind is the area of the cavity that is near the flavin site. This situation would position the amine substrate in a productive binding orientation for catalytic oxidation. There are two tyrosyl residues that are approximately perpendicular to the flavin and parallel to one another and function as an "aromatic cage" at the active site.[54c] The amine group of the substrate must approach the flavin through this path. The catalytic significance of the aromatic cage is still not completely understood. According to Edmondson *et al.*,[54c] one possible function of this aromatic cage is to orient the amine substrate to the flavin. The aromatic cage may also enhance the nucleophilicity of the amine functional group, hence increasing the reactivity of amine towards flavin. This possibility is under theoretical investigation by our group. Besides, π-stacking interactions with the aromatic side-chains may be important if the substrate involves an aromatic ring, such as in benzylamine. For the *p*-substituted benzylamine substrates used in this work, the influence of the enzyme active site discussed above is likely to be similar for all substrates since they differ from one another only at the *para* position.

Table 10 Total electronic energies (E_{el}), activation energy (ΔE^*), reaction energy (ΔE), and binding energy (ΔE_b) in atomic units[a] including zero point vibrational energy (ZPE) corrections, calculated from B3LYP/6-31G* optimization

	E_{el}	E_{el} + ZPE
Flavin,FAD, (E)	−754.167069	−754.010113
Benzylamine (S)	−326.906415	−326.759766
Flavin anion, FAD^-	−754.831936	−754.665479
Benzyl immonium (P)	−326.074382	−325.937659
Reactant complex (RC)	−1081.080596	−1080.775851
Transition state (TS)	−1081.034233	−1080.734516
Product complex (PC)	−1081.054902	−1080.749779
ΔE^* ($E_{TS1} - E_{E+S}$)	0.039250 (24.629)	0.035363 (22.190)
ΔE ($E_{product\ complex} - E_{E+S}$)	0.018582 (11.660)	0.020101 (12.613)
E_b ($E_{E+S} - E_{reactant\ complex}$)	0.007112 (4.463)	0.005971 (3.747)

[a] Unit in parenthesis is kcal mol^{-1}.

Conclusion

PM3 calculations for the polar nucleophilic mechanism show that electron-withdrawing groups at the *para* position of benzylamine increase the reaction rate. A good correlation was obtained between the log of calculated rate constants and the electronic parameter (σ) of the substituent. These results agree with the previous kinetic experiments on the effect of *p*-substituents on the reduction of MAO-A by benzylamine analogs, which has a ρ value of +2. In addition, our calculated rate constants for the polar nucleophilic mechanism showed a correlation with the rate of flavin reduction in MAO-A but no correlation with that in MAO-B. These theoretical findings support the proposed polar nucleophilic mechanism for MAO-A. It is expected that this conclusion is correct because it does not rely on quantitative accuracy. The correlation with experimental data also indicates the performance of PM3 for this type of reaction. On the other hand, the reason for the lack of correlation between theory and experiment for the MAO-B data may be the lack of consideration of steric constraints on the orientation of the aromatic ring of the substrate exerted by the side groups at the active site. The fact that

these steric factors may be dominant over electronic factors for MAO-B catalysis is suggested by available structural data.[54b]

We have also checked the performance of PM3 on the same reaction. Test calculations using DFT and *ab initio* theories produced results that were in agreement with the PM3 results, indicating that PM3 could be used to investigate this kind of reaction in the active site of enzymes. The only significant difference is that the intermediate is more stable on the PM3 potential energy surface. It is possible that the intermediate can become more stable in the active site.

Nonexistence of an intermediate on the B3LYP/6-31G* energy surface implies that adduct formation and dissociation may occur in the same step, accompanying proton transfer. Thus, nucleophilic addition, elimination, and proton transfer take place in an asynchronous, concerted fashion. However, it may also imply that electron transfer from benzylamine to flavin might take place without formation and successive cleavage of the N11–C4a bond. If this is the case, an asynchronous concerted SET mechanism proposed by Silverman (Fig. 2) may also be operating. Further work is required to distinguish between these two possibilities.

Acknowledgements

This work was supported by the Marmara University Scientific Research Projects Commission (BAPKO), project no: FEN.YY.032/032/140604. The authors thank Professor D. E. Edmondson, Emory University, Atlanta, for valuable discussions during the course of this work. We are also grateful to Professor M. T. Saçan, Boğaziçi University, Istanbul, and Mehmet Ali Akyüz for their help in preparing this manuscript.

References

1 X. Lu, M. Rodrigues, W. Gu and R. B. Silverman, *Bioorg. Med. Chem.*, 2003, **11**, 4423.
2 J. L. Ives, Heym and J. Annu, *Rep. Med. Chem.*, 1989, **24**, 21.
3 V. W. Tetrud and J. W. Langston, *Science*, 1989, **245**, 519.
4 R. B. Silverman, *Acc. Chem. Res.*, 1995, **28**, 335 and the references therein.
5 R. Sduremmo, S. Lahger, J. Perez and G. Racagani, *Depression*, 1995, **2**, 119.
6 W. E. Haeley, W. P. Burkard, A. M. Cesura, R. Kettler, H. P. Lorez, J. R. Martin, J. G. Richards, R. Scherschilicht and M. Da Prada, *Psychopharmacology (Berlin)*, 1992, **106**, 6.
7 A. M. Caesura and A. Fletcher, *Prog. Drug. Res.*, 1992, **38**, 171.
8 C. Binda, P. Newton-Vinson, F. Hubalek, D. E. Edmondson and A. Mattevi, *Nat. Struct. Biol.*, 2002, **9**, 22.
9 (*a*) R. B. Silverman, in *Advances in Electron Transfer Chemistry*, ed. P. S. Mariano, JAI Press Inc., Greenwich, 1992, vol. 2, p. 177; (*b*) N. S. Scrutton, *Nat. Prod. Rep.*, 2004, **21**, 722.
10 (*a*) Z. C. Ding, X. Lu, K. Nishimure and R. B. Silverman, *J. Med. Chem.*, 1993, **36**, 1711; (*b*) S. E. J. Rigby, R. M. G. Hynson, R. R. Ramsay, A. W. Munro and N. S. Scrutton, *J. Biol. Chem.*, 2005, **280**, 4627.
11 J. R. Miller, D. E. Edmondson and C. B. Grissom, *J. Am. Chem. Soc.*, 1995, **117**, 7830.
12 (*a*) X. Lu, M. Rodriguez, H. Ji, R. B. Silverman, A. P. B. Vintem and R. R. Ramsay, in *Flavins and Flavoproteins 2002*, ed. S. Chapman, R. Perham and N. Scrutton, Rudolf Weber Agency for Scientific Publications, Berlin, 2002, p. 817; (*b*) A. P. B. Vintem, N. T. Price, R. B. Silverman and R. R. Ramsay, *Bioorg. Med. Chem.*, 2005, **13**, 3487.
13 (*a*) C. Binda, F. Hubalek, M. Li, D. E. Edmondson and A. Mattevi, *FEBS Lett.*., 2004, 1; (*b*) J. Ma, M. Yoshimura, E. Yamashita, A. Nakagawa, A. Ito and T. Tsukihara, *J. Mol. Biol.*, 2004, **338**, 103.
14 J. R. Miller and D. E. Edmondson, *Biochemistry*, 1999, **38**, 13670.
15 M. C. Walker and D. E. Edmondson, *Biochemistry*, 1994, **33**, 7088.
16 P. Newton-Vinson and D. E. Edmondson, in *Flavins & Flavoproteins*, ed. S. Ghisla, P. Kroneck, P. Macheroux and H. Sund, Agency for Scientific Publications, Germany, 1999, p. 431.
17 C. Franot, S. Mabic and N. Castagnoli, Jr., *Bioorg. Med. Chem.*, 1997, **5**, 1519.
18 D. E. Edmondson, A. K. Bhattacharyya and M. C. Walker, *Biochemistry*, 1993, **32**, 5196.
19 R. R. Ramsay and D. J. B. Hunter, *Biochim. Biophys. Acta*, 2002, **1601**, 178.
20 D. J. Mitchell, D. Nikolic, R. B. Van Breemen and R. B. Silverman, *Bioorg. Med. Chem. Lett.*, 2001, **11**, 1757.
21 J. R. Miller and D. E. Edmondson, *J. Am. Chem. Soc.*, 1995, **117**, 7830.
22 X. Lu, M. Rodriguez, W. Gu and R. B. Silverman, *Bioorg. Med. Chem.*, 2003, **11**, 4423.
23 R. K. Nandigima, P. Newton-Vinson and D. E. Edmondson, *Biochem. Pharmacol.*, 2002, **63**, 865.
24 K. Yelekci, X. Lu and R. B. Silverman, *J. Am. Chem. Soc.*, 1989, **111**, 1138.
25 V. J. DeRose, J. C. G. Woo, W. P. Hawe, B. M. Hoffman, R. B. Silverman and K. Yelekci, *Biochemistry*, 1996, **35**, 11085.
26 K. A. Van Houten, J.-M. Kim, M. A. Bogdan, D. C. Ferri and P. S. Mariano, *J. Am. Chem. Soc.*, 1998, **120**, 5864.
27 R. B. Silverman, J. M. Cesarone and X. Lu, *J. Am. Chem. Soc.*, 1993, **115**, 4955.
28 R. B. Silverman and Y. Zelechonok, *J. Org. Chem.*, 1992, **57**, 6373.
29 R. B. Silverman, X. Lu, J. J. P. Zhou and A. Swihart, *J. Am. Chem. Soc.*, 1994, **116**, 11590.
30 R. B. Silverman, C. Z. Ding, J. L. Borillo and J. T. Chang, *J. Am. Chem. Soc.*, 1993, **115**, 2982.
31 R. B. Silverman, J. J. P. Zhou, C. Z. Ding and X. Lu, *J. Am. Chem. Soc.*, 1995, **117**, 12895.
32 R. B. Silverman and X. Lu, *J. Am. Chem. Soc.*, 1994, **116**, 4129.
33 X. Wang and R. B. Silverman, *J. Org. Chem.*, 1998, **63**, 7357.
34 C. Z. Ding and R. B. Silverman, *J. Enzyme Inhib.*, 1992, **6**, 223.
35 K. Nishimura, X. Lu and R. B. Silverman, *J. Med. Chem.*, 1993, **36**, 446.
36 C. Z. Ding, X. Lu, K. Nishimura and R. B. Silverman, *J. Med Chem.*, 1993, **36**, 1711.
37 R. B. Silverman, K. Nishimura and X. Lu, *J. Am. Chem. Soc.*, 1993, **115**, 4949.
38 R. B. Silverman, J. P. Zhou and P. E. Eaton, *J. Am. Chem. Soc.*, 1993, **115**, 8841.
39 R. B. Silverman and C. Z. Ding, *J. Am. Chem. Soc.*, 1993, **115**, 4571.
40 C. Z. Ding and R. B. Silverman, *J. Med. Chem.*, 1993, **36**, 3606.
41 (*a*) D. E. Edmondson, A. K. Bhattacharrya and J. Xu, *Biochim. Biophys. Acta*, 2000, **1479**, 52; (*b*) R. K. Nandigama and D. E. Edmondson, *Biochemistry*, 2000, **39**, 15258.
42 (*a*) M. Martin, F. Sanz, M. Campillo, L. Pardo, J. Perez and J. Turmo, *Int. J. Quantum Chem.*, 1983, **23**, 1627; (*b*) M. Martin, F. Sanz, M. Campillo, L. Pardo, J. Perez and J. Turmo, *Int. J. Quantum Chem.*, 1983, **23**, 1643.
43 (*a*) R. B. Silverman and W. P. Hawe, *J. Enzyme Inhib.*, 1995, **9**, 203; (*b*) M.-J. Huang, D. Doerge, N. Bodor, E. Pop and M. E. Brewster, *Int. J. Quantum Chem., Quantum Biol. Symp.*, 1995, **22**, 171.
44 (*a*) S. S. Erdem and K. Yelekci, *J. Mol. Struct.(Theochem)*, 2001, **572**, 97; (*b*) S. L. Palmer, S. Mabic and N. Castagnoli, Jr., *J. Med. Chem.*, 1997, **40**, 1982; (*c*) D. M. Gasparro, D. R. P. Almeida, L. F. Pisterzi, J. R. Juhasz, B. Viskolcz, B. Penke and I. G. Csizmadia, *J. Mol. Struct. (Theochem)*, 2003, **666–667**, 527.
45 J. J. P. Stewart, *J. Comput. Chem.*, 1989, **10**, 209.
46 (*a*) D. Xu, Y. Wei, J. Wu, D. Dunaway-Mariano, H. Guo, Q. Cui and J. Gao, *J. Am. Chem. Soc.*, 2004, **126**, 13649; (*b*) L. S. Devi-Kesavan, M. Garcia-Viloca and J. Gao, *Theor. Chim. Acta.*, 2003, **109**, 133; (*c*) M. D. Toney, *Biochemistry*, 2001, **40**, 1378; (*d*) B. Mattheus de Roode, H. Zuilhof, M. C. R. Franssen, A. van der Padt and A. de Groot, *J. Chem. Soc., Perkin Trans. 2*, 2000, 2217; (*e*) J. R. Alvarez-Idaboy, R. Gonzalez-Jonte, A. Hernandez-Laguna and Y. G. Smeyers, *J. Mol. Struct. (Theochem)*, 2000, **504**, 13; (*f*) J. Andres, V. S. Safont, J. B. L. Martins, A. Beltran and V. Moliner, *J. Mol. Struct. (Theochem)*, 1995, **330**, 411; (*g*) Y. Zheng and T. C. Bruice, *J. Am. Chem. Soc.*, 1997, **119**, 3868.
47 (*a*) L. Ridder, A. J. Mulholland, I. M. C. M. Rietjens and J. Vervoort, *J. Am. Chem. Soc.*, 2000, **122**, 8728; (*b*) L. Ridder, A. J. Mulholland, J. Vervoort and I. M. C. M. Rietjens, *J. Am. Chem. Soc.*, 1998, **120**, 7641; (*c*) M. Meyer, G. Wohlfahrt, J. Knablein and D. Schomburg, *J. Comput.*

Aided Mol. Des., 1998, **12**, 425; (*d*) J. Andres, V. Moliner, V. S. Safont, L. R. Domingo and M. T. Picher, *J. Org., Chem.*, 1996, **61**, 7777.
48 J. J. P. Stewart, in *Reviews in Computational Chemistry*, vol. 1, ed. K. B. Lipkowitz and B. Boyd, VCH, New York, 1996, p. 45.
49 M. J. Frisch, G. W. Trucks, H. B. Schlegel, G. E. Scuseria, M. A. Robb, J. R. Cheeseman, V. G. Zakrzewski, J. A. Montgomery, Jr., R. E. Stratmann, J. C. Burant, S. Dapprich, J. M. Millam, A. D. Daniels, K. N. Kudin, M. C. Strain, O. Farkas, J. Tomasi, V. Barone, M. Cossi, R. Cammi, B. Mennucci, C. Pomelli, C. Adamo, S. Clifford, J. Ochterski, G. A. Petersson, P. Y. Ayala, Q. Cui, K. Morokuma, D. K. Malick, A. D. Rabuck, K. Raghavachari, J. B. Foresman, J. Cioslowski, J. V. Ortiz, A. G. Baboul, B. B. Stefanov, G. Liu, A. Liashenko, P. Piskorz, I. Komaromi, R. Gomperts, R. L. Martin, D. J. Fox, T. Keith, M. A. Al-Laham, C. Y. Peng, A. Nanayakkara, M. Challacombe, P. M. W. Gill, B. Johnson, W. Chen, M. W. Wong, J. L. Andres, C. Gonzalez, M. Head-Gordon, E. S. Replogle and J. A. Pople, *Gaussian, Inc., Pittsburgh PA*, 1998.
50 D. Becke, *J. Chem. Phys.*, 1993, **98**, 5648.
51 (*a*) C. Gonzalez and H. B. Schlegel, *J. Chem. Phys.*, 1989, **90**, 2154; (*b*) C. Gonzalez and H. B. Schlegel, *J. Phys. Chem.*, 1990, **94**, 5523.
52 J. W. Ochterski, http://www.gaussian.com/g_whitepap/thermo.htm.
53 Y. J. Zeng and R. L. Ornstein, *J. Am. Chem. Soc.*, 1996, 9402.
54 (*a*) N. S. Scrutton, *Nat. Prod. Rep.*, 2004, **21**, 722; (*b*) C. Binda, M. Li, F. Hubalek, N. Restelli, D. E. Edmondson and A. Mattevi, *Proc. Natl. Acad. Sci. USA*, 2003, **100**, 9750; (*c*) D. E. Edmondson, A. Mattevi, C. Binda, M. Li and F. Hubalek, *Curr. Med. Chem.*, 2004, **11**, 1983.
55 W. J. Hehre, J. Yu, P. E. Klunzinger and L. Lou, *A Brief Guide to Molecular Mechanics and Quantum Chemical Calculations, Wavefunction*, US, 1998, p. 77.
56 B. Kallies and R. Mitzner, *J. Mol. Model*, 1995, **1**, 68.
57 D. E. Edmondson, C. Binda and A. Mattevi, *NeuroToxicology*, 2004, **25**, 63.
58 J. Dong, P. R. Carey, Y. Wei, L. Luo, X. Lu, R.-Q. Liu and D. Dunaway-Mariano, *Biochemistry*, 2002, **41**, 7453.

